2D chaotic path planning for autonomous vehicles

Roman Voliansky[1,*,†], Nina Volianska[1,†] and Arief Bramanto Wicaksono Putra[2,†]

[1] National Technical University of Ukraine "Igor Sikorsky Kyiv Polytechnic Institute", Polytechnichna Str., 37, Kyiv, 03056, Ukraine

[2] Politeknik Negeri Samarinda, Str. Jl. Cipto Mangun Kusumo, 75242, Samarinda, Indonesia

Abstract

Our paper is devoted to solution of path-planning problem for various autonomous vehicles. We offer to solve this problem by assuming that state variables of a dynamical system, which is considered as trajectory generator, are defined in some coordinate system. This coordinate system is interconnected with the target coordinate system where the path planning problem is solved. The use of an intermediate coordinate system makes it possible to form the desired path by defining transformations from one coordinate system to another. Since a number of such transformations can be very huge, an enormous number of dynamical systems can be obtained from one initial one. In our paper, we use a polar-like coordinate system as an intermediate one and we use trigonometrical functions to define interrelations between polar and orthogonal coordinate systems. All used coordinate systems are the simplest two-dimensional ones and we show the methodology of dynamical system transformation from one coordinate system to another. At the same time, one can easily increase the number of the initial state variables and extend our approach from plane to space. We prove the benefits of our approach by considering the Duffing pendulum as a dynamical system that is defined in polar coordinates and then we use various transformation routines to design a chaotic dynamical system in the orthogonal coordinate system. These routines are based on the use of various affine transformations of pendulum state variables. As a result, various chaotic attractors are being formed to use as the desired paths for unmanned vehicles.

Keywords

chaotic system, chaotic path planning, coordinate transform, autonomous vehicle

1. Introduction

Chaotic path planning is an innovative approach to trajectory generation [1, 2, 3] that leverages the principles of chaos theory [4] to create non-linear, unpredictable paths [5, 6]. Unlike conventional deterministic [7, 8] or random path planning methods [9, 10], chaotic path planning [11] introduces complex dynamics that result in extensive coverage and adaptability, making it particularly useful for applications in robotics, autonomous vehicles, and exploration.

CMSE'24: International Workshop on Computational Methods in Systems Engineering, June 17, 2024, Kyiv, Ukraine

* Corresponding author.

† These authors contributed equally.

voliansky@ua.fm (R. Voliansky); ninanin@i.ua (N.Volianska); ariefbram@gmail.com (A.B.W. Putra)

0000-0001-5674-7646 (R. Voliansky); 0000-0001-5996-2341 (N. Volianska); 0000-0003-1187-5040 (A.B.W. Putra)

Chaos theory deals with systems that exhibit sensitive dependence on initial conditions [12, 13, 14], leading to behavior that appears random despite being deterministic. This characteristic is harnessed in chaotic path planning to generate paths that are both unpredictable and thorough. Commonly used chaotic systems include the logistic map [15], the Henon map [16], the Lorenz system [17], and the Chua circuit [18, 19, 20] each providing distinct patterns of chaos that can be tailored to specific application needs. Last decades lots of papers have appeared in the scientific press to show studies [21, 22, 23, 24], designs [25, 26, 27], and usage of various chaotic systems [28, 29, 30].

The primary motivation behind chaotic path planning is to achieve superior area coverage and unpredictability. In autonomous robotic systems, this translates to more efficient exploration, improved obstacle avoidance, and enhanced security against pattern recognition by adversaries [31, 32]. For instance, robotic vacuum cleaners can utilize chaotic paths to ensure thorough cleaning, while surveillance drones can unpredictably patrol areas to prevent detection [33, 34].

In practice, chaotic path planning involves the following steps:

- Initialization: Selection of a chaotic system and definition of initial conditions [35, 36, 37].
- Sequence Generation: Iteration of the chaotic map or solving differential equations to produce a sequence of points [38, 39].
- Path Construction: The connection of these points to form a continuous path, adjusted in real-time for obstacle avoidance and environmental changes [40, 41].

It is clearly understood that the solution of the third task depends on coordinate systems where a chaotic system is defined. Many authors consider the system motion in the conventional orthogonal coordinate system [42]. Nevertheless, the huge number of such systems' attractors are known and that is why the vehicle that is moving along them can be intercepted.

We offer to avoid this drawback of chaotic path planning routine by using some coordinate transformation to define system dynamics in various coordinates.

Our paper is organized as follows: firstly, we show the possibility of attractor changing by studying system dynamics in various coordinate systems. Then we design the generalized chaotic system by considering transformation from polar to cartesian coordinates. At third, we study the peculiarities of chaotic systems implementation by using discrete-time devices. At fourth, we consider an example of a chaotic path planning system's design and study.

2. Method

2.1. Second order dynamical system motions in polar coordinates

Let us consider the simplest second order dynamical system which motion is described as follows

$$\dot{y}_1 = y_2; \quad \dot{y}_2 = -y_1. \tag{1}$$

If one starts to study (1) with phase plane method he obtains very trivial linear oscillations (Figure 1a) and phase trajectories (Figure 1b).

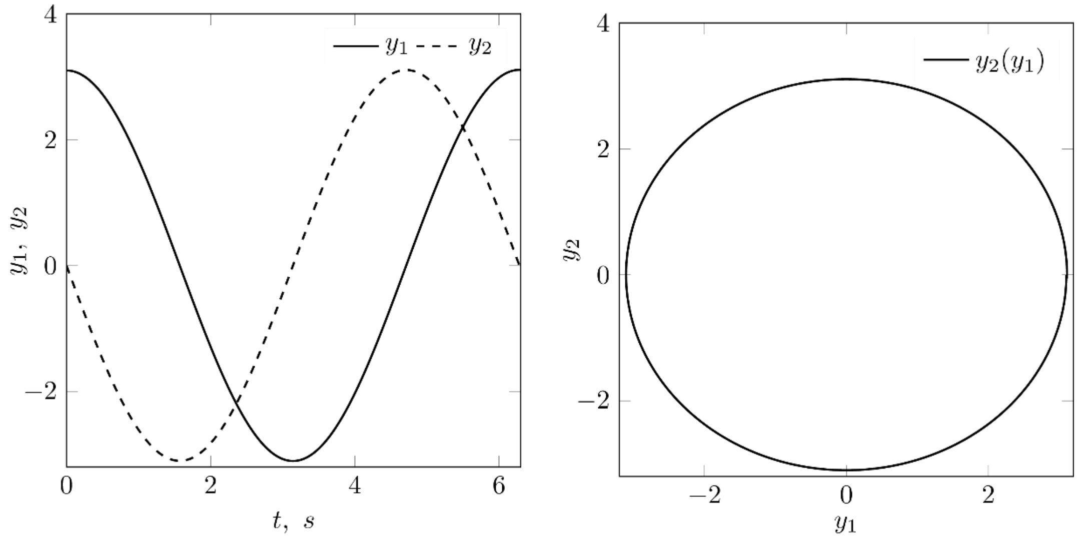

a) System time response **b)** System phase portrait

Figure 1: System simulation results.

Due to the simplicity of the above-given oscillations one can use (1) in various applications including planning of circle motions for any devices.

It is necessary to say that in the classical control theory studying of all dynamical systems are performed by using the orthogonal cartesian coordinates and assuming that system state variables make some orthogonal basis in the system state space.

It is clear that the above-mentioned coordinates are not the only possible ones and studying of system motions depend on how to interpret the system state variables and which coordinate basis they form.

Generally speaking, one can use any coordinates to describe system motions in it. It is clearly understood that such changing of the system of coordinate cause occurring of phase portraits which differ from known existing one. That is why we offer to perform such coordinate transformations to solve path planning problems and design novel motion trajectories which can be used as paths for some autonomous vehicles.

In our paper we consider system state variables as coordinates which are given in a polar system of coordinates and their generalizations. Thus, one of system state variable is considered as a linear position of some body. This position can be considered as distance ρ from some origin 0 to a representing point A and another represent angular position φ of the considered body (Figure 2). In the Figure 2 we assume that linear position is represented by y_1 and angular one is y_2, it is necessary to say that fore the system (1) it does not matter how to interpret each state variable because they have similar values and forms but differ with initial phase. For more complex system it can produce different phase portraits.

It is clear that polar and orthogonal cartesian coordinates interrelates each other with well-known dependencies, which can be written down for considered case in such a way

$$x_1 = y_1 \cos(y_2)\,; \quad x_2 = y_1 sin(y_2). \qquad (2)$$

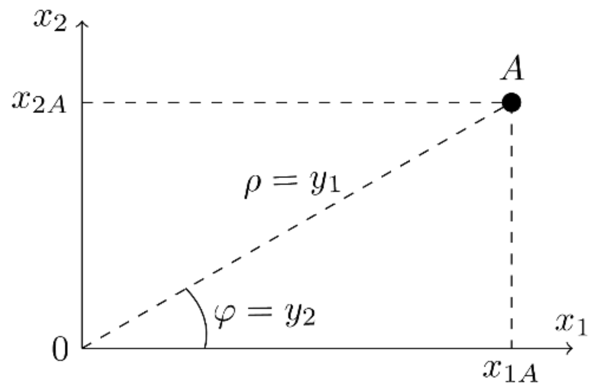

Figure 2: State variables interpretation in polar coordinates.

Results of numerical solution of (1) and (2) are shown in Figure 3.

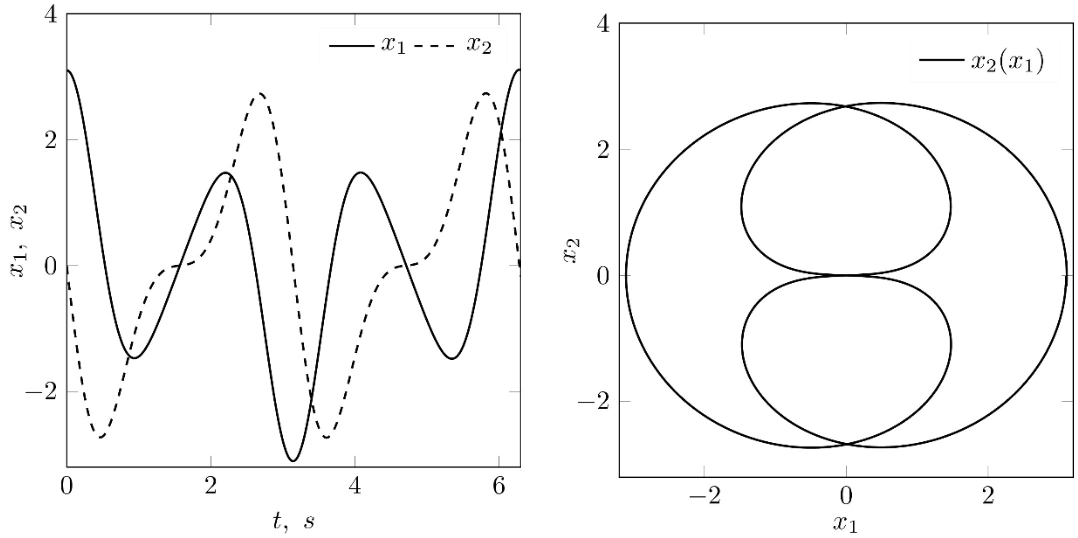

a) System time response **b)** System phase portrait

Figure 3: Output variables of dynamical system (1) and (2) with initial condition $y_1(0)=\pi$.

It is clear that shown in Figure 3 simulation results more complex than given in Figure 1 and allow to form more complex motion trajectories. Moreover, because the use of trigonometric functions oscillations become nonlinear and depend values of y_2 state variable. System output variables have different form and amplitude.

Because of the use of nonlinear function, the considered system depends on initial conditions. In Figure 4, we show simulation results for (1) with twice reduced initial value of y_1 variable.

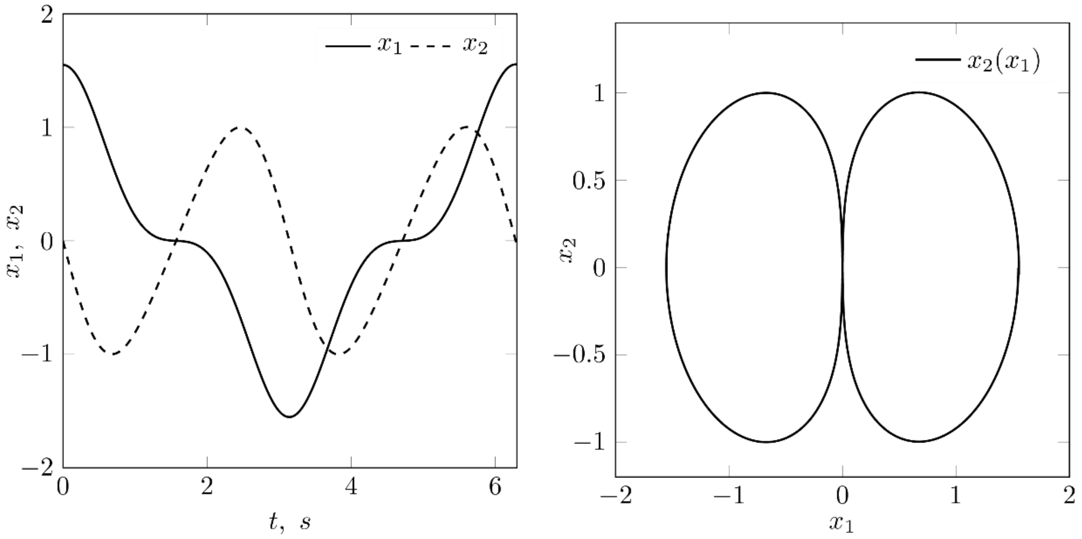

a) System time response **b)** System phase portrait

Figure 4: Output variables of dynamical system (1) and (2) with initial condition $y_1(0)=\pi/2$.

Analysis of simulation results from Figure 3 and Figure 4 allows us to claim that considering of system state variables in polar coordinates allows to design nonlinear dynamical system which can be used to produce motions path which are tremendously differ from those which are produced buy interpreting state variables in orthogonal cartesian coordinates.

2.2. The Generalized Motion in the Orthogonal Coordinate Basis

Analysis of curves which are studied by using polar coordinate system shows that in the most general case distance ρ is considered as function of body angular position φ. We claim that the opposite is also true, so angular position φ can depend on linear one ρ. This assumption gives us the possibility to generalize (2) as follows

$$x_1 = f_1(y_1, y_2)\cos\big(f_2(y_1, y_2)\big); \quad x_2 = f_1(y_1, y_2)\sin\big(f_2(y_1, y_2)\big). \tag{4}$$

From control theory viewpoint (1) and (3) form dual channel dynamical system which motion is defined by following operator equations

$$x_1 = f_1(y_1, y_2)\, cos\big(f_2(y_1, y_2)\big); \quad x_2 = f_1(y_1, y_2)\, sin\big(f_2(y_1, y_2)\big); \tag{5}$$
$$sy_1 = sy_1(0) + y_2; \quad sy_2 = sy_2(0) - y_1,$$

where s is a Laplace operator and $y_1(0)$, $y_2(0)$ are initial values of system state variable.

One can find block-diagram of such system in Figure 5.

Contrary to the initial dynamical system (1) which is considered as core system and that block-diagram is shown in dashed rectangular, the dynamical system (5) can be considered as a dual channel system. The parallel channels of this system are designed by using trigonometric expressions with nonlinear generalized arguments which depend on initial dynamical system state variables.

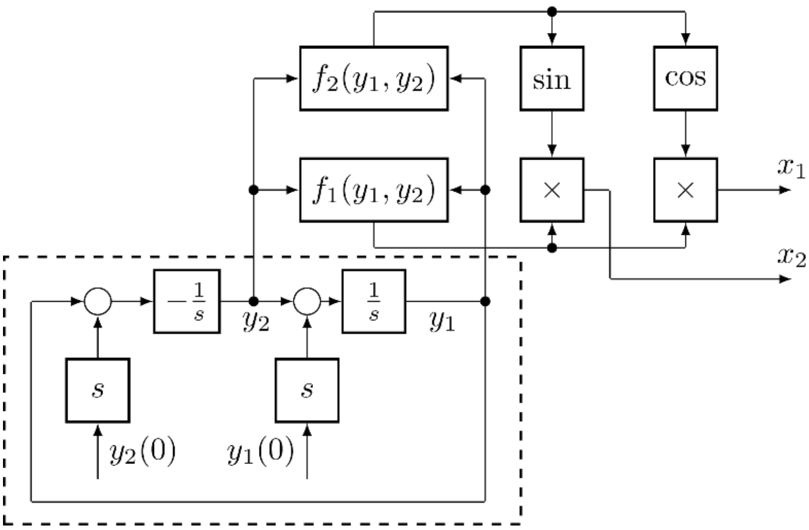

Figure 5: Scheme of the generalized dynamical system.

Since the dynamical system which is shown in Figure 5 is described with differo-algebraic equations it causes some inconveniences to use control theory methods to study systems of such type.

We offer to avoid this fact and rewrite (5) by using differential equations only. To do this we differentiate (4) by time

$$\dot{x}_1 = \left(\frac{\partial f_1(y_1,y_2)}{\partial y_1} y_2 - \frac{\partial f_1(y_1,y_2)}{\partial y_2} y_1\right)\cos\big(f_2(y_1,y_2)\big) + \tag{6}$$

$$+f_1(y_1,y_2)\left(\frac{\partial f_2(y_1,y_2)}{\partial y_2} y_1 - \frac{\partial f_2(y_1,y_2)}{\partial y_1} y_2\right)\sin\big(f_2(y_1,y_2)\big);$$

$$\dot{x}_2 = \left(\frac{\partial f_1(y_1,y_2)}{\partial y_1} y_2 - \frac{\partial f_1(y_1,y_2)}{\partial y_2} y_1\right) sin(\,f_2(y_1,y_2)) +$$

$$+f_1(y_1,y_2)\left(\frac{\partial f_2(y_1,y_2)}{\partial y_2} y_1 - \frac{\partial f_2(y_1,y_2)}{\partial y_1} y_2\right)\cos\big(f_2(y_1,y_2)\big).$$

It is clear that the use of (6) requires to have input signals y_1 and y_2 which are produced by dynamical system (1). Thus, one can consider (1) as the generator of harmonic signals for nonlinear dual channel transformation system (6). The main drawback of such system is interrelations between channels by input signals. This drawback does not allow to perform trajectory calculations by using (6) in parallel way for each channel because it is necessary to obtain common inputs.

We offer to avoid this drawback and improve system performance by redefining motion for each channel with two differential equations. That is why we offer to differentiate x_1 and x_2 output variable for two times.

$$\dot{x}_1 = \left(\nabla f_1(y_1,y_2)\cos\left(f_2(y_1,y_2)\right) - \nabla f_2(y_1,y_2) f_1(y_1,y_2)\sin\left(f_2(y_1,y_2)\right)\right)\begin{pmatrix} y_2 \\ -y_1 \end{pmatrix}; \quad (7)$$

$$\ddot{x}_1 = \left(\nabla f_1(y_1,y_2)\cos\left(f_2(y_1,y_2)\right) - \nabla f_2(y_1,y_2) f_1(y_1,y_2)\sin\left(f_2(y_1,y_2)\right)\right)\begin{pmatrix} -y_1 \\ -y_2 \end{pmatrix} +$$
$$\left(\nabla^2 f_1(y_1,y_2)\cos\left(f_2(y_1,y_2)\right) - 2\nabla f_1(y_1,y_2)\nabla f_2(y_1,y_2)\sin\left(f_2(y_1,y_2)\right) -\right.$$
$$\left. - f_1(y_1,y_2)\left(\nabla^2 f_2(y_1,y_2)\sin\left(f_2(y_1,y_2)\right) + \left(\nabla f_2(y_1,y_2)\right)^2 cos\left(f_2(y_1,y_2)\right)\right)\right)\begin{pmatrix} y_2 \\ -y_1 \end{pmatrix}.$$

$$\dot{x}_2 = \left(\nabla f_1(y_1,y_2)\sin\left(f_2(y_1,y_2)\right) + \nabla f_2(y_1,y_2) f_1(y_1,y_2)\cos\left(f_2(y_1,y_2)\right)\right)\begin{pmatrix} y_2 \\ -y_1 \end{pmatrix}; \quad (8)$$

$$\ddot{x}_2 = \left(\nabla f_1(y_1,y_2)\sin\left(f_2(y_1,y_2)\right) + \nabla f_2(y_1,y_2) f_1(y_1,y_2)\cos\left(f_2(y_1,y_2)\right)\right)\begin{pmatrix} -y_1 \\ -y_2 \end{pmatrix} +$$
$$\left(\nabla^2 f_1(y_1,y_2)\sin\left(f_2(y_1,y_2)\right) + 2\nabla f_1(y_1,y_2)\nabla f_2(y_1,y_2)\cos\left(f_2(y_1,y_2)\right) +\right.$$
$$\left. + f_1(y_1,y_2)\left(\nabla^2 f_2(y_1,y_2)\cos\left(f_2(y_1,y_2)\right) - \left(\nabla f_2(y_1,y_2)\right)^2 sin\left(f_2(y_1,y_2)\right)\right)\right)\begin{pmatrix} y_2 \\ -y_1 \end{pmatrix}.$$

Equations (6) and (7) define motion of the considered system in the orthogonal cartesian coordinates by assuming that y_1 and y_2 are given polar coordinates. Nevertheless, one can use the first equation in (7) and (8) as well as (4) to solve inverse problem for the considered dual channel dynamical system and define y_i as function of x_i.

Such a solution depends on functions $f_i(y_1, y_2)$ and in the most general case can be defined as follows

$$y_1 = g_{11}(x_1, \dot{x}_1) = g_{21}(x_2, \dot{x}_2); \quad y_2 = g_{12}(x_1, \dot{x}_1) = g_{22}(x_2, \dot{x}_2), \quad (9)$$

where $g_{ij}(\cdot)$ are nonlinear functions which are inverse to functions $f_1(y_1, y_2)$ and $f_2(y_1, y_2)$.

If one substitutes (9) into the last equations of (7) and (8), he can rewrite these equations in such a way

$$\ddot{x}_1 = q_{11}(x_1, \dot{x}_1)\cos\left(q_{12}(x_1, \dot{x}_1)\right) + q_{13}(x_1, \dot{x}_1) cos\left(q_{12}(x_1, \dot{x}_1)\right); \quad (10)$$

$$\dot{x}_2 = q_{21}(x_2, \dot{x}_2)\cos\left(q_{22}(x_2, \dot{x}_2)\right) + q_{23}(x_2, \dot{x}_2) cos\left(q_{12}(x_2, \dot{x}_2)\right), \quad (11)$$

where $q_{ij}(\cdot)$ are some nonlinear functions which are obtained after substituting (9) into (7) and (8) and performing algebraic simplifications.

The proposed approach allows us to define two independent nonlinear 2nd order differential equations which allows to define components of acceleration of moved body which motion is defined in the orthogonal coordinate basis.

It is clearly understood that these components define projections of moved body acceleration vector and its length can be found in a trivial way

$$a = \sqrt{\ddot{x}_1^2 + \ddot{x}_2^2}. \quad (12)$$

One can use (12) to check if the planned motion can be physically implemented and suitable for the considered body, body speed and position can be found by integrating (10) and (11).

3. Results and Discussion

3.1. Duffing Pendulum Modeling and Simulating

It is clear that one can use both regular and chaotic dynamical system equation to define their state variables as polar coordinates in some space plane. Moreover, in case of the use chaotic systems it becomes possible to design dynamical system with predefined chaotic attractor.

Let us show the benefits of the usage of our approach by considering well-known Duffing equation

$$\dot{y}_1 = y_2;\ \ \dot{y}_2 = -a_{11}y_2 - a_{01}y_1 - a_{03}y_1^3 + b_1 cos(b_2 t), \tag{13}$$

where y_1 and y_2 are pendulum position and speed, a_{ij} are pendulum factors, b_1 and b_2 are external harmonic signal parameters.

In this paper we study Duffing pendulum with following parameters $a_{11} = 0.02$, $a_{01} = 1$, $a_{03} = 5$, $b_1 = 8$, $b_2 = 0.5$. Also, we assume zero initial conditions for the considered motion. Numerical solution of the Duffing equation (13) is shown in Figure 6.

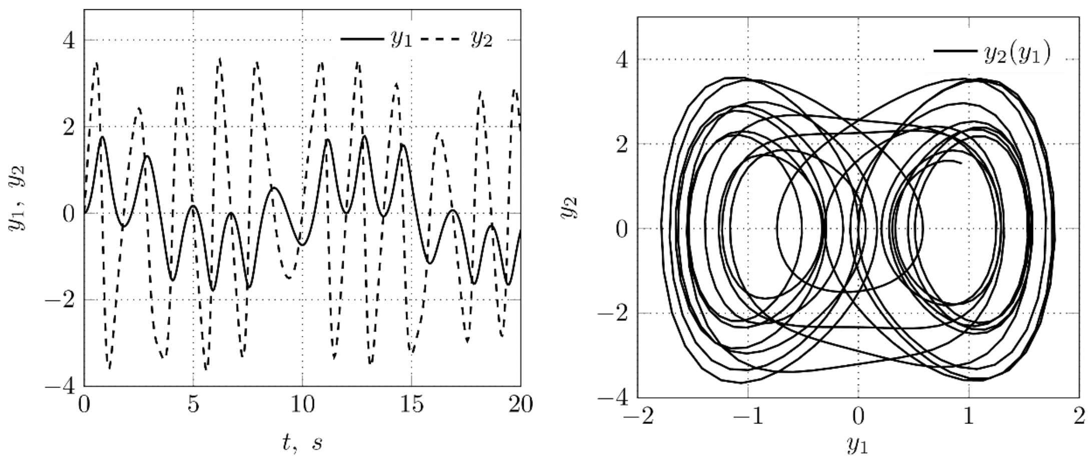

a) System time response **b)** System phase portrait

Figure 6: Numerical solution of (13).

Analysis of Figure 6 proves that under some conditions Duffing pendulum can be considered as chaotic dynamical system with external harmonic excitation. Figure 6 makes the initial base to compare with novel results. Due to the features of attractor in Figure 6b we call it as infinity-like attractor. It necessary to say that the Duffing pendulum is considered because of this is a one of simplest second order chaotic systems. Nevertheless, one can use any chaotic system as the core to perform the above-given transformations.

3.2. Duffing Pendulum Dynamic in Polar Coordinates

3.2.1. The Simplest Polar to Cartesian Coordinate Transformations

At first, we consider the simplest case of the proposed approach use. In this case we assume that core dynamical system is defined as (13) and transformation expressions given by (2). To study the effect of interpreting system state variables we consider both cases

$$\rho = y_1; \varphi = y_2 \tag{14}$$

and

$$\rho = y_2; \varphi = y_1\ . \tag{15}$$

Simulation results for the dynamical system (13) with transformation (2) and variables (14) are shown in Figure 7 and Figure 8 illustrates results of numerical solution of (13) and (2) with variables (15).

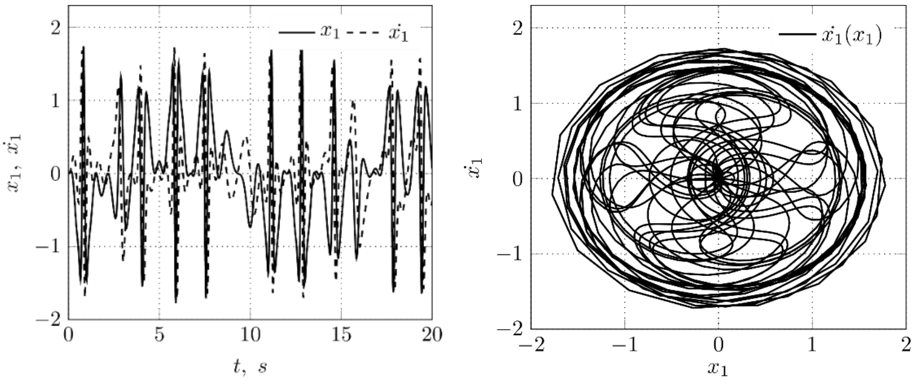

a) System time response **b)** System phase portrait

Figure 7: Numerical solution of (13) with transformations (2) and variables (14).

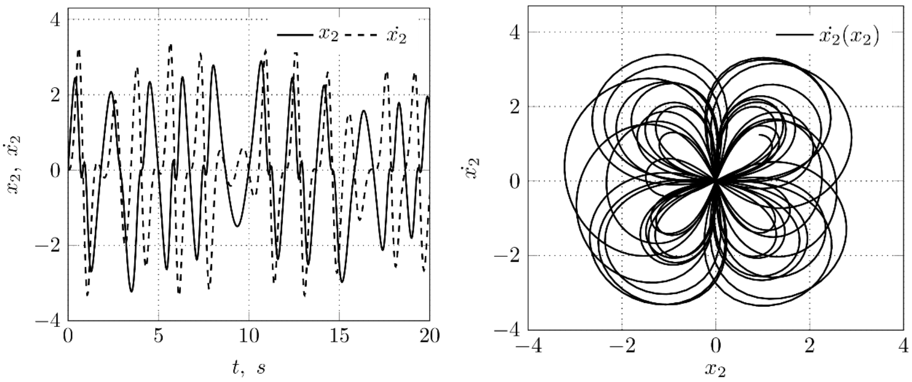

a) System time response **b)** System phase portrait

Figure 8: Numerical solution of (13) with transformations (4) and variables (15).

Analysis of given in Figure 7 and Figure 8 simulation results allows us to claim that interpretation of Duffing pendulum state variables as variables in polar coordinates with following transformation into orthogonal coordinates allows us to dramatically change Duffing pendulum attractor and form of its oscillations. Moreover, the use y_1 as pendulum linear position and y_2 as its angular position gives us the possibility to increase the nonlinearity of oscillations and make them more complex. At the same time, the use of y_2 as pendulum linear position and y_1 as its linear one makes pendulum oscillation less nonlinear. In both cases pendulum attractors differ from the initial one. Furthermore, the assuming that pendulum variables are defined in polar coordinates avoid occurring of dual scroll attractors and produce novel attractors for this dynamical system which we call as eye-like for given in Figure 7b attractor and clover-like attractor for attractor which is given in Figure 8b.

3.2.2. The Affine Polar to Cartesian Coordinate Transformations

Now we make transformations (14) and (15) more complex and assume that the pendulum linear position in polar coordinates is defined as linear combination of Duffing pendulum state variables and its angular position is unchanged

$$\rho = y_1 + y_2; \varphi = y_2 \tag{16}$$

and

$$\rho = y_1 + y_2; \varphi = y_1. \tag{17}$$

One can find simulation results for dynamical systems which are described by (13), (16) and (13), (17) in Figure 9 and Figure 10.

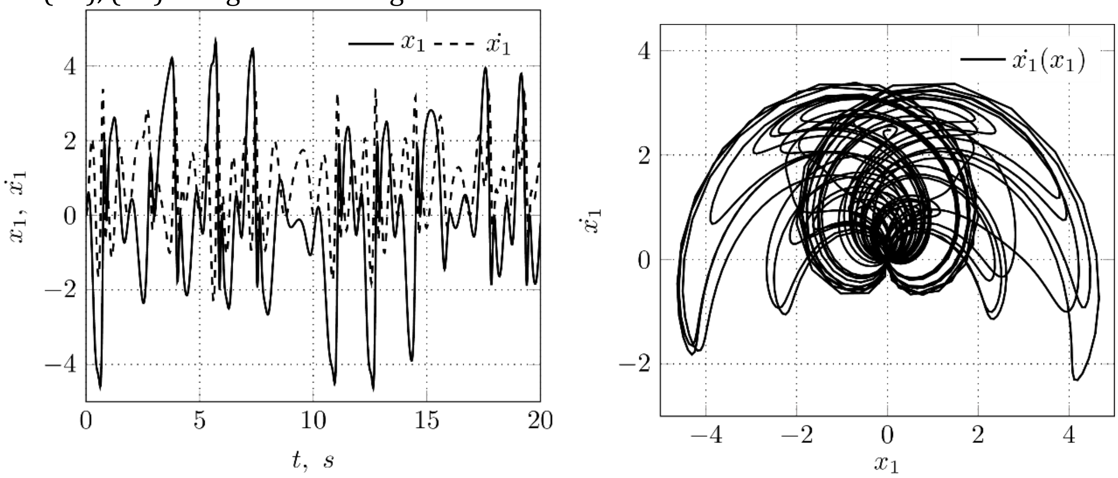

a) System time response **b)** System phase portrait

Figure 9: Numerical solution of (13) with transformations (2) and variables (16).

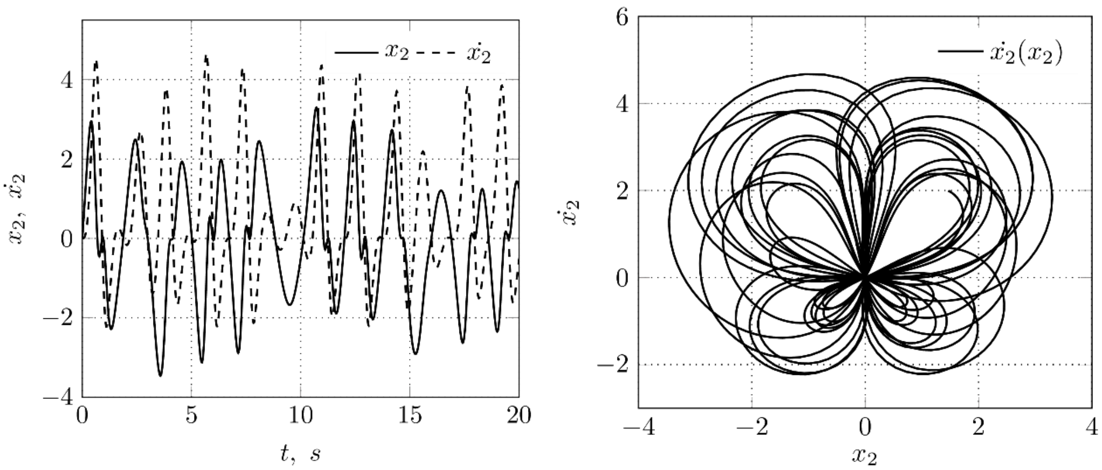

a) System time response **b)** System phase portrait

Figure 10: Numerical solution of (13) with transformations (4) and variables (17).

In Figure 11 and Figure 12 we show simulation results for the case when linear pendulum position is defined by only one pendulum state variable and its angular position is sum of pendulum state variables. In other words, following transformations are used

$$\rho = y_1; \varphi = y_1 + y_2 \tag{18}$$

and

$$\rho = y_2; \varphi = y_1 + y_2. \tag{19}$$

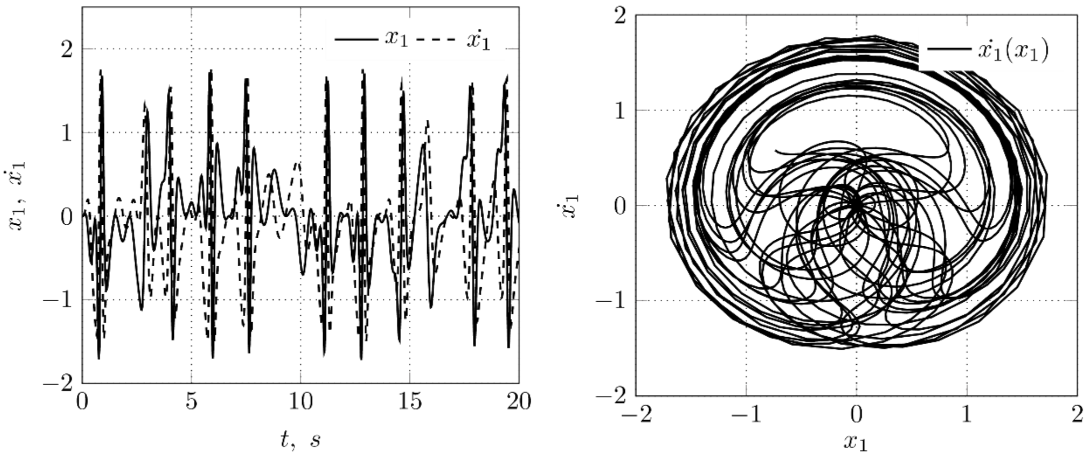

a) System time response **b)** System phase portrait

Figure 11: Numerical solution of (13) with transformations (4) and variables (18).

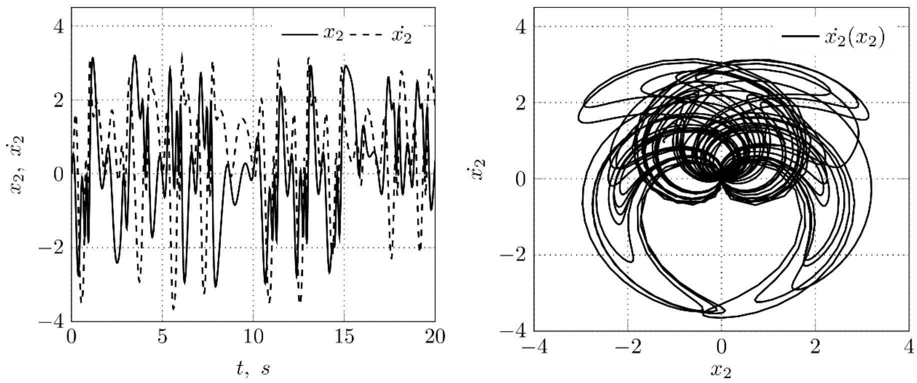

a) System time response **b)** System phase portrait

Figure 12: Numerical solution of (13) with transformations (4) and variables (19).

Analysis of given in Figure 9 – Figure 12 simulation results shows that if one defines linear combinations of Duffing pendulum state variables and then use the obtained combinations as initial signals for transformation (2) it becomes possible to change system attractors in tremendous ways.

It is necessary to say that usage of linear combinations of Duffing pendulum state variables also allows us to form hidden attractors. One of such attractors (Figure 13) can be obtained if one uses following transformation which is the combination of the two previous ones

$$\rho = y_1 + y_2; \varphi = y_1 + y_2 \,. \quad (20)$$

The main feature of the shown in Figure 13 system that in polar coordinates its linear and angular positions equal each other.

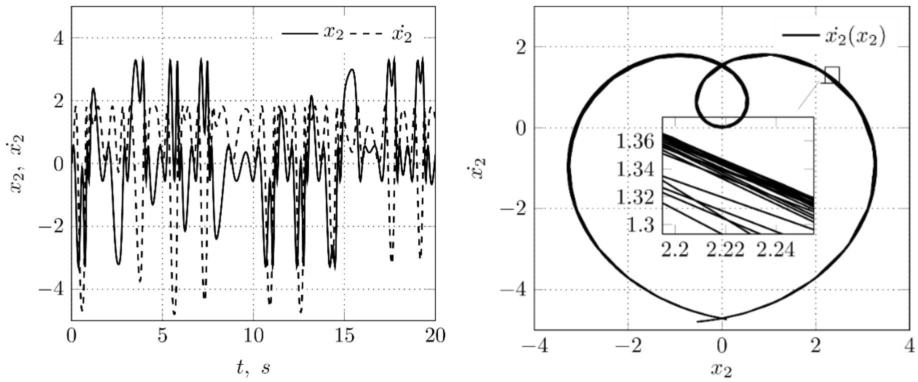

a) System time response **b)** System phase portrait

Figure 13: Numerical solution of (13) with transformations (4) and variables (20).

Such an attractor is formed because of the quite stable amplitude of chaotic oscillations in the considered system. Contrary to the above-considered systems the last one forms motion trajectories which quite close each other but motions along these trajectories becomes according to unpredictive laws.

Similar results can be obtained in special cases when one of pendulum positions is assumed as constant (Figure 14 and Figure 15)

$$\rho = r; \varphi = y_1 + y_2; \quad (21)$$

$$\rho = y_1 + y_2; \varphi = f \,. \quad (22)$$

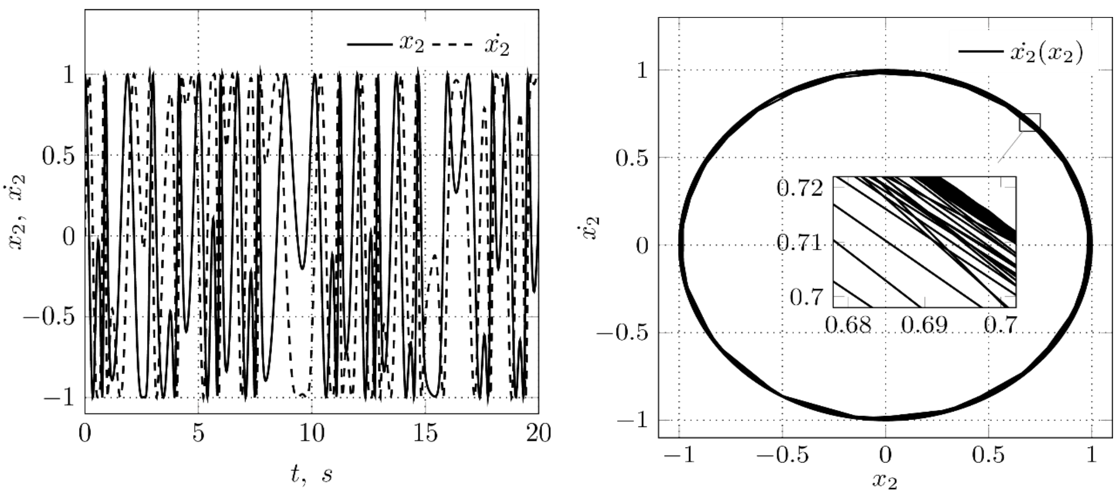

a) System time response **b)** System phase portrait

Figure 14: Numerical solution of (13) with transformations (4) and variables (21).

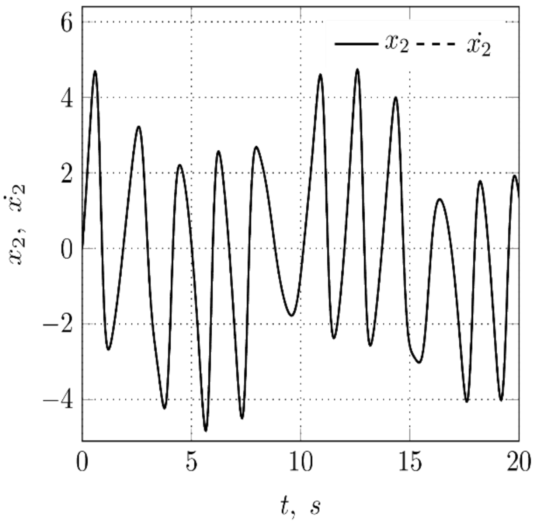

a) System time response

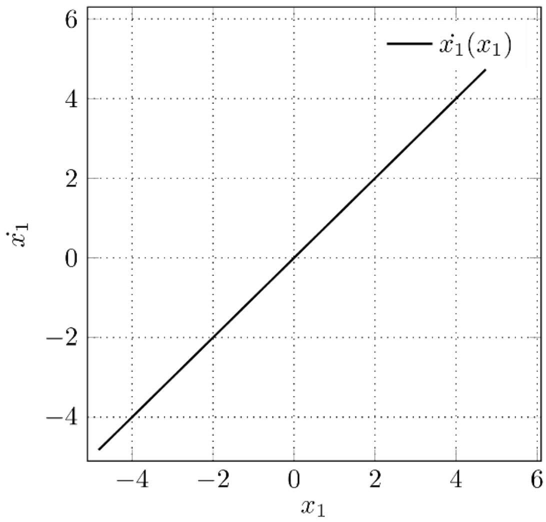

b) System phase portrait

Figure 15: Numerical solution of (13) with transformations (4) and variables (22).

Analysis of Figure 13 – Figure 15 proves the possibility of design chaotic systems with hidden attractors by using Duffing equations.

3.3. Duffing Pendulum-based Chaotic Dynamical System Design and Implementation

We design all above-considered chaotic systems by taking into account the given in previous section approach which is based on the taking into account (13) and differentiate (2) for two times for each linear and angular pendulum position in the polar coordinates.

Now let us show the system design which is based on (13), (2).

We show such a design by differentiating first expression in (2)

$$\dot{x}_1 = y_2\cos(y_2) - y_1(b_1\cos(b_2 t) - a_{11}y_2 - a_{01}y_1 - a_{03}y_1^3)\sin(y_2). \tag{23}$$

It is clear that both of expressions (2) and (23) are nonlinear for state variables y_i. That is why, we use numerical methods to solve them

$$y_1 = \frac{x_1}{cos(y_2)}; \tag{24}$$

$$y_2 = y_2 - \frac{\dot{x}_1 - y_2\cos(y_2) + x_1\left(b_1\cos(b_2 t) - a_{11}y_{2i-1} - a_{01}\frac{x_1}{cos(y_2)} - a_{03}\frac{x_1^3}{cos^3(y_2)}\right)tan(y_2)}{y_2\,sin(y_2) - cos(y_2) - x_1\left(a_{11} + \frac{a_{01}x_1\,sin(y_2)}{cos^2(y_2)} + \frac{3a_{03}x_1^3\,sin(y_2)}{cos^4(y_2)}\right)tan(y_2) - x_1\left(a_{11}y_2 + \frac{a_{01}x_1}{cos(y_2)} - \frac{a_{03}x_1^3}{cos^3(y_2)}\right)(1+tan^2(y_2))}.$$

Then we differentiate (23) one more time

$$\begin{aligned}\ddot{x}_1 = &-y_1\cos(b_2 t)^2\cos(y_2)b_1^2 + b_1((2a_{03}y_1^4 + 2a_{01}y_1^2 + 2a_{11}y_1y_2 + 1)\cos(y_2 + \\ &+\sin(y_2)(a_{11}y_1 - 2y_2))\cos(b_2 t) + y_1\sin(y_2)\sin(b_2 t)b_1b_2 - \\ &-(a_{03}y_1^4 + a_{01}y_1^2 + a_{11}y_1y_2 + 1)(a_{03}y_1^3 + a_{01}y_1 + a_{11}y_2)\cos(y_2) - \sin(y_2)\times \\ &\times(a_{03}a_{11}y_1^4 - 5a_{03}y_2y_1^3 + a_{01}a_{11}y_1^2 + a_{11}^2y_1y_2 - 3a_{01}y_1 - 2a_{11}y_2^2).\end{aligned} \tag{25}$$

and substitute into the second derivative (25) values of y_1 and y_2 from (24).

Other equations are defined in the similar way. We offer to use numerical approximation of derivative operator with feedback differences

$$\frac{d}{dt} \approx \frac{1-z^{-1}}{z^{-1}T}, \qquad (26)$$

where z^{-1} is a shift operator and T is a discretization time to implement (25) and similar equations in the digital devices.

To perform transformation of (25) in discrete-time form, let us rewrite it as follows

$$\dot{x}_{11} = x_{12}; \qquad (27)$$

$$\begin{aligned}\dot{x}_{12} = &-y_1 \cos(b_2 t)^2 \cos(y_2) b_1^2 + b_1((2a_{03}y_1^4 + 2a_{01}y_1^2 + 2a_{11}y_1y_2 + 1)\cos(y_2)) \\ &+\sin(y_2)(a_{11}y_1 - 2y_2))\cos(b_2 t) + y_1 \sin(y_2)\sin(b_2 t) b_1 b_2 \\ &- (a_{03}y_1^4 + a_{01}y_1^2 + a_{11}y_1y_2 + 1)(a_{03}y_1^3 + a_{01}y_1 \\ &+ a_{11}y_2)\cos(y_2) \\ &- \sin(y_2)(a_{03}a_{11}y_1^4 - 5a_{03}y_2y_1^3 + a_{01}a_{11}y_1^2 + 3y_2a_{11}^2y_1 \\ &- y_2a_{01}y_1 - 2a_{11}y_2^2)\end{aligned}$$

and apply (26)

$$x_{11} = z^{-1}x_{11} + Tz^{-1}x_{12}; \qquad (28)$$

$$\begin{aligned}x_{12} = &z^{-1}x_{12} + z^{-1}T(b_1(()2a_{03}y_1^4 + 2a_{01}y_1^2 + 2a_{11}y_1y_2 + 1)\cos(y_2) - \\ &y_1\cos(b_2t)^2\cos(y_2)b_1^2 + +\sin(y_2)(a_{11}y_1 - 2y_2))\cos(b_2t) + \\ &y_1\sin(y_2)\sin(b_2t)b_1b_2 - (a_{03}y_1^4 + a_{01}y_1^2 + a_{11}y_1y_2 + 1)(a_{03}y_1^3 + a_{01}y_1 + \\ &a_{11}y_2)\cos(y_2) - \sin(y_2)(a_{03}a_{11}y_1^4 - 5a_{03}y_2y_1^3 + a_{01}a_{11}y_1^2 + 3y_2a_{11}^2y_1 - \\ &y_2a_{01}y_1 - 2a_{11}y_2^2)).\end{aligned}$$

One can use modern CPU/MCU/FPGA devices to implement the designed chaotic system.

4. Conclusions

The interpreting of dynamical system state variables as coordinates in some coordinate system which is different from the orthogonal cartesian one gives us the possibility to define novel dynamical systems with novel oscillations and attractors. One can transform these attractors into a conventional orthogonal cartesian coordinate system by using various transformation expressions. The use of these transformations allows us to define a multichannel dynamical system and bind each channel with corresponding coordinates to define body position in the plane for each time moment. Combining these moments gives us the possibility to define the desired trajectory for a considered body. Different transformation allows us to determine different paths for a vehicle and use them in various applications.

One can use both regular and chaotic systems as core systems to implement our approach. In the case of chaotic system usage, one can get various chaotic systems, in which attractors have features that can be useful in one or another application.

The above-considered systems are designed and studied by using linear combinations of Duffing pendulum state variables. Even in this case, the transformed system is defined with quite complex equations due to the trigonometric function use and system nonlinearity. This fact requires to use of numerical methods to complete the coordinate transformation. We believe that replacing nonlinear functions with piecewise linear ones makes it possible to simplify transformation from one coordinate system to another and avoid the use of numerical methods. We see the check of this hypothesis as one of the future developments of our work. One more possible problem to solve by using the proposed approach is studying dynamical systems with nonlinear combinations of their state variables. Also, one can use the proposed approach to design multidimensional dynamical systems that have attractors in some N-th dimensional coordinate systems.

References

[1] T. Zha, Y. Li, L. Sun, A local planning method based on minimum snap trajectory generation and traversable region for inspection of airport roads, in: Proceeding of 5th International Conference on Automation, Control and Robots (ICACR), Nanning, China, 2021, pp. 38–42. doi: 10.1109/ICACR53472.2021.9605163.

[2] K. Liu et al., Optimal time trajectory generation and tracking control for over-actuated multirotors with large-angle maneuvering capability, IEEE Robotics and Automation Letters 7 (3) (2022) 8339–8346. doi: 10.1109/LRA.2022.3187260.

[3] O. A. Sushchenko, V. O. Golitsyn, Data processing system for altitude navigation sensor, in: Proceeding of IEEE 4th International Conference on Methods and Systems of Navigation and Motion Control (MSNMC 2016), Kyiv, Ukraine, 2013, pp. 84–87. doi: 10.1109/MSNMC.2016.7783112.

[4] A. Ascoli, A. S. Demirkol, R. Tetzlaff, L. Chua, Edge of chaos theory resolves smale paradox, IEEE Transactions on Circuits and Systems I: Regular Papers 69 (3) (2022) 1252–1265. doi: 10.1109/TCSI.2021.3133627.

[5] R. Li, Path planning for service robots, in: Proceeding of 5th World Conference on Mechanical Engineering and Intelligent Manufacturing (WCMEIM), Ma'anshan, China, 2022, pp. 850–853. doi: 10.1109/WCMEIM56910.2022.10021507.

[6] L. Han, X. Wu, X. Sun, Hybrid path planning algorithm for mobile robot based on A* algorithm fused with DWA, in: Proceeding of IEEE 3rd International Conference on Information Technology, Big Data and Artificial Intelligence (ICIBA), Chongqing, China, 2023, pp. 1465–1469. doi: 10.1109/ICIBA56860.2023.10165386.

[7] O. Sushchenko, V. Chikovani, H. Tsiruk, Redundant information processing techniques comparison for differential vibratory gyroscope, Eastern-European Journal of Enterprise Technologies 4 (7(82)) (2016) 45–52.

[8] L. Zhiteckii, V. Azarskov, K. Solovchuk, O. Sushchenko, Discrete-time robust steady-state control of nonlinear multivariable systems: A unified approach, IFAC Proceedings Volumes 47 (3) (2014) 8140–8145, 2014. doi: 10.3182/20140824-6-ZA-1003.01985.

[9] S. Al-Ansarry, S. Al-Darraji, A. Shareef, D. G. Honi, F. Fallucchi, Bi-directional adaptive probabilistic method with a triangular segmented interpolation for robot path planning in complex dynamic-environments, IEEE Access 11 (2023) 87747–87759. doi: 10.1109/ACCESS.2023.3290897.

[10] M. Walid, M. M. Elnaggar, W. S. Sayed, L. A. Said, A. G. Radwan, A comparative study of different chaotic systems in path planning for surveillance applications, in: Proceeding of International Conference on Microelectronics (ICM), New Cairo City, Egypt, 2021, pp. 25–28. doi: 10.1109/ICM52667.2021.9664903.

[11] P. Das, P. P. Singh, A 4D chaotic system with seventeen equilibria: Synchronization and anti-synchronization, in: Proceeding of 1st International Conference on Power Electronics and Energy (ICPEE), Bhubaneswar, India, 2021, pp. 1–6. doi: 10.1109/ICPEE50452.2021.9358496.
[12] R. D. Syah, S. Madenda, R. J. Suhatril and S. Harmanto, Hybrid digital image cryptography using composition of Henon map transposition and logistic map substitution, in: Proceeding of IEEE International Conference of Computer Science and Information Technology (ICOSNIKOM), Laguboti, North Sumatra, Indonesia, 2022, pp. 1–6. doi: 10.1109/ICOSNIKOM56551.2022.10034926.
[13] O.A. Sushchenko, Y.N. Bezkorovainyi, N.D. Novytska, Nonorthogonal redundant configurations of inertial sensors, in: Proceeding of IEEE 4th International Conference on Actual Problems of Unmanned Aerial Vehicles Developments (APUAVD 2017), Kyiv, Ukraine, 2017, pp. 73–78. doi: 10.1109/APUAVD.2017.8308780.
[14] O. A. Sushchenko, Y. M. Bezkorovainyi, V.O. Golytsin, Processing of redundant information in airborne electronic systems by means of neural networks, in: Proceeding of IEEE 39th International Conference on Electronics and Nanotechnology, Kyiv, Ukraine, 2019, pp. 652–655. doi: 10.1109/ELNANO.2019.8783394.
[15] Z. Galias, Dynamics of the Hénon map in the digital domain, IEEE Transactions on Circuits and Systems 70 (1) (2023) 388–398. doi: 10.1109/TCSI.2022.3217139.
[16] Y. Jiang, C. Li, Z. Liu, T. Lei, G. Chen, Simplified memristive Lorenz oscillator, IEEE Transactions on Circuits and Systems II: Express Briefs 69 (7) (2022) 3344–3348. doi: 10.1109/TCSII.2022.3169013
[17] R. Voliansky, O. Sadovoi, Y. Sokhina, I. Shramko, M. Pushkar, Chua’s circuit with time-depended variable capacitances and its synchronization, in: Proceeding of IEEE International Scientific-Practical Conference Problems of Infocommunications, Science and Technology (PIC S&T), Kyiv, Ukraine, 2019, pp. 794–798. doi: 10.1109/PICST47496.2019.9061531.
[18] R. Voliansky, A. Sadovoi, Chua's circuits interval synchronization, in: Proceeding of 4th International Scientific-Practical Conference Problems of Infocommunications, Science and Technology (PIC S&T), Kharkov, Ukraine, 2017, pp. 439–443. doi: 10.1109/INFOCOMMST.2017.8246434.
[19] F. Capligins, A. Litvinenko, A. Aboltins, D. Kolosovs, FPGA implementation and study of synchronization of modified Chua’s circuit-based chaotic oscillator for high-speed secure communications, in: Proceeding of IEEE 8th Workshop on Advances in Information, Electronic and Electrical Engineering (AIEEE), Vilnius, Lithuania, 2021, pp. 1–6. doi: 10.1109/AIEEE51419.2021.9435783.
[20] R. Voliansky, O. Kluev, O. Sadovoi, O. Sinkevych, N. Volianska, Chaotic time-variant dynamical system, in: Proceeding of IEEE 15th International Conference on Advanced Trends in Radioelectronics, Telecommunications and Computer Engineering (TCSET), Lviv-Slavske, Ukraine, 2020, pp. 606–609. doi: 10.1109/TCSET49122.2020.235503.
[21] S. Vaidyanathan, A. Sambas, G. G. Devadhas, P. S. G. Anand, A new 2-scroll chaos plant with multistability and its circuit realization, in: Proceeding of 2nd International Conference on Intelligent Computing Instrumentation and Control Technologies (lCICICT), 2019, pp. 1638–1642.

[22] M. S. Papadopoulou, V. Rusyn, A. D. Boursianis, P. Sarigiannidis, K. Psannis, S. K. Goudos, Diverse implementations of the Lorenz system for teaching non-linear chaotic circuits, in: Proceeding of IEEE International Conference on Information, Communication and Networks, Xi'an, China, 2021, pp. 416–420. doi: 10.1109/ICICN52636.2021.9674018.
[23] D. Cirjulina, R. Babajans, D. Kolosovs, A. Litvinenko, Fundamental frequency impact on Colpitts chaos oscillator dynamics, in: Proceeding of Workshop on Microwave Theory and Technology in Wireless Communications (MTTW), Riga, Latvia, 2023, pp. 19–23. doi: 10.1109/MTTW59774.2023.10320021.
[24] M. S. Hasan, P. S. Paul, M. Sadia, M. R. Hossain, Design of a weighted average chaotic system for robust chaotic operation, in: Proceeding of IEEE International Midwest Symposium on Circuits and Systems (MWSCAS), Lansing, MI, USA, 2021, pp. 954–957. doi: 10.1109/MWSCAS47672.2021.9531758.
[25] L. Moysis et al., A novel chaotic system with application to secure communications, in: Proceeding of International Conference on Modern Circuits and Systems Technologies, Bremen, Germany, 2020, pp. 1–4. doi: 10.1109/MOCAST49295.2020.9200286.
[26] S. Vaidyanathan, E. Tlelo-Cuautle, A. Sambas, F. Grasso, A new nonlinear dynamical model with three quadratic nonlinear terms and hidden chaos, in: Proceeding of 42nd International Convention on Information and Communication Technology, Electronics and Microelectronics (MIPRO), Opatija, Croatia, 2019, pp. 153–156. doi: 10.23919/MIPRO.2019.8757210.
[27] O. Holubnychyi, M. Zaliskyi, I. Ostroumov, O. Sushchenko, O. Solomentsev, Y. Averyanova, et al., Self-organization technique with a norm transformation based filtering for sustainable infocommunications within CNS/ATM systems, in: I. Ostroumov, M. Zaliskyi (Eds.), Proceedings of the International Workshop on Advances in Civil Aviation Systems Development. Lecture Notes in Networks and Systems, Springer, Cham, 2024, vol. 992, pp. 262–278. doi: 10.1007/978-3-031-60196-5_20.
[28] O. Solomentsev, M. Zaliskyi, O. Holubnychyi, I. Ostroumov, O. Sushchenko, Y. Bezkorovainyi, et al., Efficiency analysis of current repair procedures for aviation radio equipment, in: I. Ostroumov, M. Zaliskyi (Eds.), Proceedings of the International Workshop on Advances in Civil Aviation Systems Development. Lecture Notes in Networks and Systems, Springer, Cham, 2024, vol. 992, pp. 281–295. doi: 10.1007/978-3-031-60196-5_21.
[29] I. Haddad, A. Belmeguenai, D. Herbadji, S. Boumerdassi, A new encryption approach for color image using 3D fractional order chaotic system, in: Proceeding of IEEE International Conference on Sciences and Techniques of Automatic Control and Computer Engineering (STA), Sousse, Tunisia, 2022, pp. 391–394. doi: 10.1109/STA56120.2022.10019142.
[30] A. B. Phillips et al., Autosub 2000 under ice: Design of a new work class AUV for under ice exploration, in: Proceeding of IEEE/OES Autonomous Underwater Vehicles Symposium (AUV), St. Johns, NL, Canada, 2020, pp. 1–8. doi: 10.1109/AUV50043.2020.9267952.
[31] F. Fanelli, D. Fenucci, R. Marlow, M. Pebody, A. B. Phillips, Development of a multi-platform obstacle avoidance system for autonomous underwater vehicles, in:

Proceeding of IEEE/OES Autonomous Underwater Vehicles Symposium (AUV), St. Johns, NL, Canada, 2020, pp. 1–6. doi: 10.1109/AUV50043.2020.9267942.
[32] S. Richhariya, K. Wanaskar, S. Shrivastava, J. Gao, Surveillance drone cloud and intelligence service, in: Proceeding of 11th IEEE International Conference on Mobile Cloud Computing, Services, and Engineering (MobileCloud), Athens, Greece, 2023, pp. 1–10. doi: 10.1109/MobileCloud58788.2023.00007.
[33] S. K. V et al., Silent surveillance autonomous drone for disaster management and military security using artificial intelligence, in: Proceeding of 3rd International Conference on Innovative Practices in Technology and Management (ICIPTM), Uttar Pradesh, India, 2023, pp. 1–4, doi: 10.1109/ICIPTM57143.2023.10118136.
[34] J. Zhou, W. Zhang, Y. Feng, B. O. Onasanya, Control selection based on state change of chaotic system, in: Proceeding of IEEE International Conference on Computer and Communications, Chengdu, China, 2022, pp. 2357–2363, doi: 10.1109/ICCC56324.2022.10065738.
[35] Z. Wang, Y. Pei, A Study on Multi-objective chaotic evolution algorithms using multiple chaotic systems, in: Proceeding of IEEE 10th International Conference on Awareness Science and Technology (iCAST), Morioka, Japan, 2019, pp. 1–6. doi: 10.1109/ICAwST.2019.8923329.
[36] R. Voliansky, I. Ostroumov, O. Sushchenko, Y. Averyanova, O. Solomentsev, O. Holubnychyi, M. Zaliskyi, et. al. Variable-structure interval-based duffing oscillator, in: Proceeding of IEEE 42nd International Conference on Electronics and Nanotechnology (ELNANO), 2024, pp. 581–586.
[37] T. M. Hoang, Perturbed chaotic map with varying number of iterations and application in image encryption, in: Proceeding of IEEE Eighth International Conference on Communications and Electronics (ICCE), Phu Quoc Island, Vietnam, 2021, pp. 413–418. doi: 10.1109/ICCE48956.2021.9352070.
[38] I. Á. Harmati, L. T. Kóczy, Notes on the dynamics of hyperbolic tangent fuzzy cognitive maps, in: Proceeding of IEEE International Conference on Fuzzy Systems (FUZZ-IEEE), New Orleans, LA, USA, 2019, pp. 1–6. doi: 10.1109/FUZZ-IEEE.2019.8858950.
[39] O. Sushchenko, Y. Bezkorovainyi, O. Solomentsev, M. Zaliskyi, O. Holubnychyi, I. Ostroumov, et. al., Algorithm of determining errors of gimballed inertial navigation system, In: O. Gervasi, et al. (Eds.), Computational Science and Its Applications – ICCSA 2024, Lecture Notes in Computer Science, Vol. 14813, 2024, pp. 1–13.
[40] Z. Zhang, R. Jia, X. Chen, S. Shao, Dynamic obstacle avoidance path planning of unmanned vehicle based on improved APF, in: Proceeding of 7th International Symposium on Computer Science and Intelligent Control (ISCSIC), Nanjing, China, 2023, pp. 135–140. doi: 10.1109/ISCSIC60498.2023.00037.
[41] F. Wang, R. Wang, H. H. C. Iu, C. Liu, T. Fernando, A novel multi-shape chaotic attractor and its FPGA implementation, IEEE Transactions on Circuits and Systems II: Express Briefs 66 (12) (2019) 2062–2066. doi: 10.1109/TCSII.2019.2907709.
[42] Y. Yang, L. Huang, N. V. Kuznetsov, Q. Lai, Design and implementation of grid-wing hidden chaotic attractors with only stable equilibria, IEEE Transactions on Circuits and Systems I: Regular Papers 70 (12) (2023) 5408–5420. doi: 10.1109/TCSI.2023.3312489.